ANNALS OF
BOTANY
Founded 1887

Mechanical traits of fine roots as a function of topology and anatomy

Zhun Mao[1,#,*], Yan Wang[2,#], M. Luke McCormack[3,4], Nick Rowe[1], Xiaobao Deng[2,5],
Xiaodong Yang[2], Shangwen Xia[2], Jérôme Nespoulous[1], Roy C. Sidle[6], Dali Guo[3] and Alexia Stokes[1]

[1]AMAP, INRA, CNRS, IRD, CIRAD, University of Montpellier, Montpellier, France, [2]Key Laboratory of Tropical Forest Ecology, Xishuangbanna Tropical Botanical Garden, Chinese Academy of Sciences, Mengla, Yunnan 666303, China, [3]Center of Forest Ecosystem Studies and Qianyanzhou Station, Key Laboratory of Ecosystem Network Observation and Modeling, Institute of Geographic Sciences and Natural Resources Research (IGSNRR), Chinese Academy of Sciences (CAS), Beijing 100101, China, [4]Department of Plant and Microbial Biology, University of Minnesota, St Paul, MN 55108, USA, [5]Xishuangbanna Station for Tropical Rain Forest Ecosystem Studies, Chinese Ecosystem Research Net, Mengla, Yunnan 666303, China and [6]Sustainability Research Centre, University of the Sunshine Coast, Maroochydore, Queensland, Australia.
*For correspondence. E-mail maozhun04@126.com
#These authors have contributed equally to this work.

• **Background and Aims** Root mechanical traits, including tensile strength (T_r), tensile strain (ε_r) and modulus of elasticity (E_r), are key functional traits that help characterize plant anchorage and the physical contribution of vegetation to landslides and erosion. The variability in these traits is high among tree fine roots and is poorly understood. Here, we explore the variation in root mechanical traits as well as their underlying links with morphological (diameter), architectural (topological order) and anatomical (stele and cortex sizes) traits.
• **Methods** We investigated the four tropical tree species *Pometia tomentosa*, *Barringtonia fusicarpa*, *Baccaurea ramiflora* and *Pittosporopsis kerrii* in Xishuangbanna, Yunnan, China. For each species, we excavated intact, fresh, fine roots and measured mechanical and anatomical traits for each branching order.
• **Key Results** Mechanical traits varied enormously among the four species within a narrow range of diameters (<2 mm): <0.1–65 MPa for T_r, 4–1135 MPa for E_r and 0.4–37 % for ε_r. Across species, T_r and E_r were strongly correlated with stele area ratio, which was also better correlated with topological order than with root diameter, especially at interspecific levels.
• **Conclusions** Root topological order plays an important role in explaining variability in fine-root mechanical traits due to its reflection of root tissue development. Accounting for topological order when measuring fine-root traits therefore leads to greater empirical understanding of plant functions (e.g. anchorage) within and across species.

Key words: Biomechanics, tensile strength, modulus of elasticity, tensile strain, root diameter, fine roots, root topology, root anatomy.

INTRODUCTION

Plant mechanical quality impacts plant fitness, population distributions, ecological functioning and the surrounding abiotic environment (Niklas, 1992; Denny and Gaylord, 2002; Read and Stokes, 2006; Stokes *et al.*, 2009; Onoda *et al.*, 2011). Trade-offs frequently occur between mechanical traits and those related to growth and reproduction (Wright and Westoby, 2002; Read and Stokes, 2006), highlighting the key role of mechanical traits in defining plant strategies for resource acquisition and allocation. Despite their fundamental importance in defining plant form and strategy, mechanical traits are a relatively poorly understood aspect of functional plant ecology (Reich *et al.*, 1991; Wright and Westoby, 2002; Stokes *et al.*, 2009; Onoda *et al.*, 2011). In several previous studies on plant water transport, mechanical traits were often measured and associated with hydraulic and/or anatomical traits to characterize trade-offs between hydraulic conductivity and wood mechanical strength of stems (Wagner *et al.*, 1998; Domec and

Gartner, 2002; Woodrum *et al.*, 2003; Jacobsen *et al.*, 2007) and coarse roots (Pratt *et al.*, 2007). However, plant mechanical traits have been largely absent from broader plant trait analyses, which instead have primarily focused on chemical and morphological traits related to plant fitness (Wright *et al.*, 2004; Violle *et al.*, 2007; Osnas *et al.*, 2013; Roumet *et al.*, 2016). This issue is exacerbated below-ground, where the longstanding disparity between assessments of leaf traits compared with root traits has left a tremendous gap in our understanding of fine-root mechanical traits. For example, while the global patterns of interspecific mechanical trait variation have been investigated in leaves (Onoda *et al.*, 2011), the most comprehensive root trait database currently available contains no observations of key mechanical traits (Iversen *et al.*, 2017).

Root mechanical traits encompass multiple quantitative characteristics that result from differences in tissue structure and composition. Roots express specific tensile, compressive, buckling, twisting and/or bending behaviour in the soil environment

SYMBOLS

Symbol	Name	Unit	Definition
d	Root diameter	mm	By default, d is identical to mean diameter (d_{mean}); d_{max}, and d_{min} refer to the maximum and minimum diameters measured along a root.
E_r	Root modulus of elasticity	MPa	Resistance to being deformed elastically; defined as the quasi-linear part (elastic zone) of the slope when tensile stress and strain are plotted. Root material is heterogeneous; therefore E_r is an 'equivalent' elasticity characterizing the root structure.
$f(m)$	Load applied to a tested root	N	f varies with the data measurement step (m).
F	Load for failure in tension	N	F is equal to the maximum of $f(m)$ in this study.
L_0	Initial gauge length	mm	Vertical distance between the two clamps prior to a mechanical test.
m	Step of measurement	–	A step of measurements when applying a load during a mechanical test.
m_{max}	Maximum step of measurements	–	Maximum step of measurements when applying a load during a mechanical test.
T_r	Root tensile strength	MPa	Ultimate stress at root failure divided by root cross-sectional area, $T_r = F/(\pi d^2/4)$.
$\varepsilon(m)$	Strain	%	Relative extended length of a root during a mechanical test; ε varies with the data measurement step (m).
ε_r	Root tensile strain	%	Relative extended length at root failure due to tension.
$\Delta l(m)$	Root extension	mm	Root extension during a mechanical test (in mm); Δl varies with the data measurement step (m).
$\sigma(m)$	Stress	MPa	Stress a root undergoes during a mechanical test (in MPa); σ varies with the data measurement step (m), $\sigma = f/(\pi d^2/4)$.
$\dot{\sigma}(m)$	The first derivation of stress	–	The first derivative of $\sigma(m)$ along $\varepsilon(m)$.

in response to herbivory, soil compaction, movement and settling (Niklas, 1999; Bourrier *et al.*, 2013; Mao *et al.*, 2014*a*; Schwarz *et al.*, 2015; Johnson *et al.*, 2016). Mechanical traits are therefore key metrics used when studying plant anchorage and root penetration into soil (Niklas *et al.*, 2002; Chimungu *et al.*, 2015), and to assess plant functioning and development across environmental gradients (Pratt *et al.*, 2007; Genet *et al.*, 2011). Characterizing root mechanical traits is particularly important for a better understanding of physical interactions between fine roots and the soil (Wu *et al.*, 1979; Stokes *et al.*, 2009), which is required by (1) engineers and foresters using vegetation to reinforce soil to reduce landslides and erosion, (2) forest managers managing plantations subjected to wind storms, and (3) urban arborists managing trees in confined spaces or with roots growing close to infrastructures.

In biomechanical studies on fine roots, tensile strength (T_r, the load required to cause failure in tension divided by root cross-sectional area), elastic modulus (E_r, resistance to being deformed elastically) and tensile strain (ε_r, maximum deformation during tensile loading) are among the most important traits measured (Ghestem *et al.*, 2014). Of the three mechanical traits, tensile strain is the least commonly studied, although recent reports have highlighted its important role in root–soil physical interactions (Schwarz *et al.*, 2010; Ghestem *et al.*, 2014). Previous studies have found that both tensile strength and elastic modulus generally show decreasing trends with increasing diameter (Genet *et al.*, 2005; Fan and Su, 2008), although the absolute load required to cause root failure (i.e. F) is higher for coarser roots. However, variability in data is high and poorly understood, particularly in very fine roots, suggesting that diameter alone is insufficient to explain the variation observed. For example, Ghestem *et al.* (2014) showed that fine-root tensile strength measured across nine species varied by more than an order of magnitude and was not well explained by variation in root diameter. It has been suggested that cellulose or lignin content account for strength and elasticity values in fine roots (Hathaway and Penny, 1975; Genet *et al.*, 2005, 2011; Hales *et al.*, 2009; Zhang *et al.*, 2014), but such disparities in chemical composition between roots may merely be a consequence of tissue development as a function of root age. Alternatively, several studies successfully used root anatomical traits that can reflect root developmental stage or even root age to capture variability in

biomechanical traits (Hathaway and Penny, 1975; Loades *et al.*, 2013, 2015; Chimungu *et al.*, 2015). Together, these studies strongly challenge the relevance of only using root diameter to explain root mechanical traits, particularly among distal fine roots.

Despite clear benefits of linking root anatomy or chemical properties to mechanical properties, measuring these traits is time-consuming and it is desirable to find functional proxies that allow the differentiation of root development. Root topology, defined as the geometric structure of root branching orders (Berntson, 1997), has been widely used in plant ecology to understand root activity (Fitter, 1982; Pregitzer *et al.*, 1997; Guo *et al.*, 2004, 2008). Root topological order is considered a good proxy reflecting root physiological functioning, including absorption, transport and storage (Guo *et al.*, 2008), and is often strongly associated with root traits that determine the cycling of carbon, nutrients and water (McCormack *et al.*, 2015). Hishi (2007) and Guo *et al.* (2008) found that anatomical traits, such as cortex thickness and secondary xylem, differ significantly among roots within a narrow diameter interval (e.g. <2 mm) but varied more consistently based on topological branch order. Thus, interspecific comparisons of root traits or species' evolutionary histories should be more reliable when they are based on roots belonging to the same order than those belonging to the same diameter class (Kong *et al.*, 2014; Ma *et al.*, 2018). These findings suggest that introducing root topological order is a promising approach to explain the heterogeneity in mechanical traits observed among fine roots both within and across species, but to our knowledge no previous studies have yet identified the link between topology and mechanics.

We determined variation in root mechanical traits related to tensile behaviour as well as their relationships with root order, diameter and anatomy. To do this, we conducted mechanical tests on fresh fine roots collected from four common tree species in tropical China. The species varied widely in terms of life history as well as basic root morphology, anatomy and architecture. We hypothesized that (1) root diameter and topology are positively related to the force required to cause failure (F) but negatively related to tensile strength (T_r), elastic modulus (E_r) and tensile strain (ε_r); (2) relationships between traits are driven by anatomical traits, such as stele and cortex sizes; (3) explicitly accounting for root topology significantly improves predictions of mechanical traits.

MATERIALS AND METHODS

Study sites and model species

The study site was located in the Gougulin forest (21°55′ N, 101°16′ E, 580 m a.s.l.), a secondary tropical forest aged >50 years, in the Xishuangbanna Tropical Botanical Garden, Yunnan, China. Mean monthly air temperature is highest in June (21.8 °C) and lowest in January (11.0 °C) and mean annual precipitation is 1493 mm (based on 40-year averages from 1959–98; Cao *et al.*, 2006). The climate exhibits a distinct seasonal pattern with a relatively dry season from November to April and a wet season from May to October. Soils are typically laterites, which are common throughout the region (Wang *et al.*, 1996; Cao *et al.*, 2006), and are thin with a maximum depth <1.0 m.

Species richness in the forest is high, with >120 tree species. Tree canopy cover reaches 90 %, sheltering a variety of understorey species, including ~30 shrub and ~25 herbaceous species. Within the forest, we sampled roots from a 20 × 100 m² plot away from areas accessible by tourists visiting the botanical garden. The zone we sampled was situated along a west-facing slope varying from 20° to 30° across the plot.

We selected four native species that are commonly seen in forests of the area: *Pometia tomentosa* (Sapindaceae), *Barringtonia fusicarpa* (Lecythidaceae), *Baccaurea ramiflora* (Euphorbiaceae) and *Pittosporopsis kerrii* (Icacinaceae). Among them, *P. tomentosa* and *B. fusicarpa* were upper canopy species, *B. ramiflora* was an upper sub-canopy species and *P. kerrii* was a lower sub-canopy species.

Tree sampling and root excavation

For each species, individual trees were chosen at random from within the plot, provided that the following criteria were met: (1) individuals were healthy and robust, without obvious signs of disease; (2) diameter at breast height was visually judged as representative of the plot and atypically old or juvenile trees were avoided; and (3) individuals of each species were located >20 m apart. For each species, at least three individuals were sampled (except for *P. tomentosa*, for which we sampled only two trees of similar size) in mid-September 2015. For each individual sampled, we carefully excavated fine roots from around the structural roots emerging from the trunk. After intact, fine-root branches containing at least six branch orders had been identified, roots were carefully wrapped in moist paper towels and then stored in a cooler box. Roots were transported to the laboratory, where they were gently rinsed within 3 h of sampling and then stored in a refrigerator at 4 °C.

Following procedures adapted from Genet *et al.* (2005), laboratory measurements and mechanical tests were performed as soon as possible, normally within 2–5 d after sampling. An appropriate sub-sample of roots (i.e. <2 mm) was selected for each test to ensure that all the tested roots were in good condition based on their colour and texture. Any roots that appeared diseased or dead (e.g. when a root could be easily broken and its elasticity was reduced) were excluded.

Measurement of root topology and diameter

Measurement of root topology and diameter was performed prior to mechanical testing. Each root network was placed in a glass tray with 5 mm of water, and roots were carefully spread out to minimize overlap (Fig. 1). We applied Fitter's (1982) centripetal (i.e. morphometric) protocol (Berntson, 1997) to determine the root topological orders of each root network. Distal roots are considered as first-order and two joint roots of the same order (k^{th}) give the $(k + 1)^{th}$ order to their parent root (Fig. 1E).

Each of the selected roots from the root network was carefully cut for the measurement of diameter using a digital microscope (S8 APO, Leica, Germany; magnification ×8). Individual roots do not have a constant diameter, rather they often taper, are tortuous and contain nodes and roughness, all of which can render diameter highly variable along the root, even within a distance of a few millimetres (Giadrossich *et al.*, 2017). Therefore, for each root segment subjected to mechanical testing, four high-resolution photographs were taken: left of centre, centre, right of centre, and the centre again after axially rotating the root 90°. For each image, root diameter was measured twice at two randomly selected locations along the root segment. Consequently, we obtained eight measurements of root diameter per root analysed. Root cross-sectional area was calculated for a circle using the maximum (d_{max}), minimum (d_{min}) and mean (d_{mean}) diameters, respectively.

Mechanical tests and mechanical trait estimation

For each species, we randomly selected at least five healthy and undamaged roots containing at least six orders (except for *P. kerrii*, for which only four orders were included, as roots of order ≥5 had diameters that were consistently >2 mm). We then selected four to six root segments of each different root order for mechanical tests, taking care to select roots that were generally representative of the sampled species. An In-Spec 2200 BT (Instron® Corporation) tensile testing machine was used for mechanical testing. Two different force transducers of (maximum capacities of 125 and 10 N with an accuracy of 0.25 %) were used during the tests, depending on root diameter (usually 10 N for roots <0.5 mm in diameter and 125 N for the remaining roots). Each root segment was placed into rubber-lined, manually tightened grips of the Instron®; they were further fixed with strips of sandpaper and 502 Super Waterglue. The rate of success was fairly high (>80 %), probably due to the fact that we focused on fine roots. We carried out 160 successful mechanical tests (i.e. roots failed in the middle of the sample and did not slip out of or fail near the clamps; Table 1).

For each root segment tested, the initial gauge length (i.e. distance between the two grips, L_0, in mm) was at least 20 times the diameter of the root. The crosshead speed was fixed at 5.0 mm min⁻¹, which is within the typical speed range used in other studies (Giadrossich *et al.*, 2017). During each test, the Instron® software automatically captured the load (*f*, in N) and displacement (Δl, in mm), as a continuous curve with a data acquisition rate of 50 recorded points per second. The
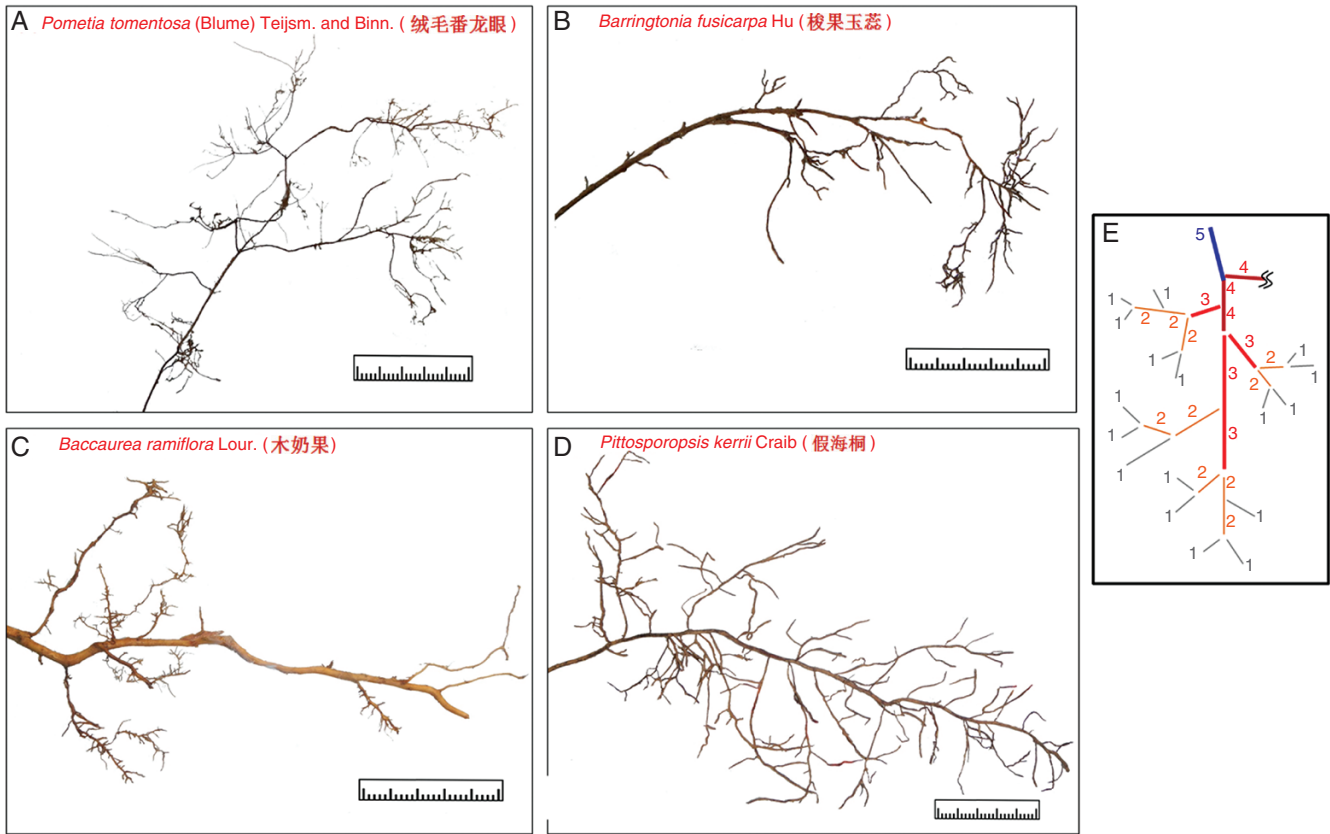
FIG. 1. Root morphology of the four tree species (A–D). (E) Centripedal (functional) segment protocol of counting root topological order (after Berntson, 1997). Scale bar graduations = 1 mm.

TABLE 1. *Linear models for predicting root mechanical traits (Y) by choosing either root diameter or topology*

Species	N	Y	Y = a × diameter + b				Y = a × topology + b			
			a	b	R^2	AIC	a	b	R^2	AIC
P. tomentosa	35	T_r	47.89***	10.22*	0.37	275	6.16***	6.62	0.34	276
		E_r	599.85*	325.5**	0.14	496	40.33	391.84**	0.04	500
		ε_r	7.13	11.88***	0.02	253	0.99	11.13**	0.03	253
B. fusicarpa	29	T_r	24.26***	−2	0.62	206	6.91***	−7.49*	0.73	196
		E_r	370.81	−25.53	0.54	373	102.75***	−99.92	0.6	369
		ε_r	5.24	13.73***	0.07	208	1.09	13.9***	0.04	209
B. ramiflora	49	T_r	17.57***	−0.96	0.69	316	5.18***	−2.49	0.41	348
		E_r	306.45***	34.51	0.47	643	85.55***	23.94	0.25	659
		ε_r	3.14	9.65***	0.08	309	1.32*	8.02***	0.09	309
P. kerrii	47	T_r	6.28***	−0.43	0.42	239	2.8***	−1.19	0.62	219
		E_r	147.59***	−23.84	0.38	543	66.88***	−44.05*	0.58	525
		ε_r	−1.32	10.41***	0.02	258	−0.38	10.1***	0.01	259

Each pair of *a* and *b* denotes the slope and intercept, i.e. the two coefficients in each model

For each row of T_r and E_r, the grey zone indicates the better model.

N, number of observations; AIC, Akaike information criterion

***$P < 0.001$; **$P < 0.01$; *$P < 0.05$.

test was stopped when the root segment ruptured due to tension (m_{max}, the maximum number of measurements made per test). Following each test, we calculated the root tensile stress and strain curve, i.e. $\sigma(m)$ over $\varepsilon(m)$ curves using eqns (1) and (2):

$$\sigma(m) = \frac{f(m)}{0.25\pi d^2} \qquad (1)$$

where *m* is the step of measurement, $1 \leq m \leq m_{max}$ (m_{max} is the maximum step of measurement per test) and *d* is root diameter;

$$\varepsilon(m) = 100\frac{\Delta l(m)}{L_0} \qquad (2)$$

where L_0 = initial gauge length (in mm).

Based on the curves of $\sigma(m)$ against $\varepsilon(m)$, the load for failure in tension (F) and the mechanical traits (T_r, ε_r, E_r) per root were then obtained. F, T_r and ε_r of a root are the ultimate tensile load, strength and strain, respectively. We used the maximum values of $f_r(m)$ and $\sigma(m)$ from a given test to identify F and T_r, respectively. The deformation rate at which a root fails (ε_r, as a percentage), is equal to $\varepsilon(m)$ when the maximum value of $\sigma(m)$, i.e. T_r, occurred. T_r could also be calculated using $F/0.25\pi d^2$.

E_r corresponds to the slope of the curve of $\sigma(m)$ against $\varepsilon(m)$ within the quasi-linear elastic stage of a root in tension, describing the rate of T_r per unit ε_r. In several previous studies (e.g. Ghestem *et al.*, 2014), the location on the curve of $\sigma(m)$ against $\varepsilon(m)$ where the slope was calculated was usually chosen visually, and this may bring subjectivity into E_r estimates. In this study, we propose the following approach to minimize this subjectivity. For each $\sigma(m)$ against $\varepsilon(m)$ curve, we calculated the first derivative of the curve (fitted by a polynomial equation) when $\varepsilon \leq \varepsilon_r$. Then, along the curve of the first derivation, i.e. the curve of $\dot{\sigma}(m)$ against $\varepsilon(m)$, we determined the peak of $\dot{\sigma}(m)$, notated as $\dot{\sigma}_k$. E_r (in MPa) is equal to $100 \times \dot{\sigma}_k$. As calculations of T_r and E_r require root diameter data, using different diameters (d_{mean}, d_{min} or d_{max}) allowed us to characterize T_r and E_r uncertainties due to root heterogeneity.

Root anatomy

Due to the destructive nature of the mechanical tests, different roots had to be used for anatomical measurements. These roots were randomly chosen from the individuals sampled, and for each species and each root order we selected at least five roots in total. To ensure that roots were representative of those used in mechanical testing, we conducted the same assessments of root diameter as those performed on roots prior to mechanical testing and confirmed that roots between the two sets of measurements were similar in terms of their root diameter and topological values (Supplementary Data Figs S1.1 and S1.2). Cross-sections were then cut by hand from fresh root material with a double-sided blade and stained in acid fuchsin. Soft materials, e.g. carrot and potato, were used to help cutting. First- and second-order roots were cut under a microscope (S8 APO, Leica, Germany). Three sections per root were chosen and placed under a microscope (DM 2000, Leica, Germany), which was connected to a computer for visualization. For each cross-section, root diameter (mm), cortex thickness (mm) and stele diameter (mm) were measured in three directions and mean values were calculated. The epidermis was included in the measurement of cortex thickness. Mean stele area ratio (mm^2/mm^2) was calculated as the cross-sectional area of the stele divided by that of the entire root, while cortex to diameter ratio (mm/mm) was calculated as the cortex radial thickness divided by the radius of the entire root. It should be noted that both stele area ratio and cortex diameter ratio are dimensionless, but the former is area-based and the latter is length-based. Digital images were analysed using public software ImageJ (Schneider *et al.*, 2012).

Statistical analyses

The traits we studied were root morphological (diameter), topological, anatomical (stele area ratio, cortex thickness and cortex diameter ratio) and mechanical (T_r, ε_r and E_r) traits. Genet *et al.* (2011) described the relationship of F against diameter by choosing a power law:

$$F = Ad^B \qquad (3)$$

where A and B are two coefficients (multiplier and scaling exponent, respectively) and d is diameter. From eqn (3) we can derive the equation for T_r:

$$T_r = \frac{F}{0.25\pi d^2} = \frac{4A}{\pi}d^{B-2} = \alpha d^\beta \qquad (4)$$

where α and β are two coefficients (multiplier and scaling exponent, respectively) that can be derived from A and B: $\alpha = \frac{4A}{\pi}$ and $\beta = B - 2$. It should be noted that eqn (4) is the routine inverse power law relationship used in most previous studies characterizing T_r with $\beta < 0$ (e.g. see Giadrossich *et al.*, 2017). In this study, we fitted eqn (3) and calibrated A and B. Given the close relationship between F and T_r in terms of calculation, here we mainly use T_r when examining relationships between traits.

We explored multiple-trait relationships using principal component analysis (PCA). Before the PCA, traits were standardized using the zero-mean approach. We also performed analysis of covariance (ANCOVA) to explain mechanical trait variability in relation to more commonly measured root traits: root diameter and topological order. In all of the analyses, diameter and anatomical traits were considered quantitative variables, while topological order was considered as either quantitative (e.g. in the ANCOVA when diameter was excluded and in the PCA) or qualitative (e.g. in the ANCOVA when diameter was included). In the latter case, root order was split as a three-level qualitative variable (orders 1–2, 3–4 and 5–6); this enabled us to compare the importance of diameter and topological order in the same model, to best explain the variability of mechanical traits. Prior to each analysis, we tested the normality and homoscedasticity of the data. Data were log-transformed in cases of non-normal distributions. We also carried out *post hoc* tests using Tukey honestly significant difference (HSD) tests to discriminate among factors. Facilitating visual data interpretation, we used the Convex hull polygon algorithm (Cormen *et al.*, 2001) to describe the occupation of the data points belonging to a species. All statistical analyses were performed using R 3.2.3 (R Core Team, 2015).

RESULTS

Root mechanical traits

Load for failure and tensile strength, i.e. F and T_r, increased significantly with increasing root diameter in all four species (Supplementary Data Fig. S1.3 for F and Fig. 2 for T_r),
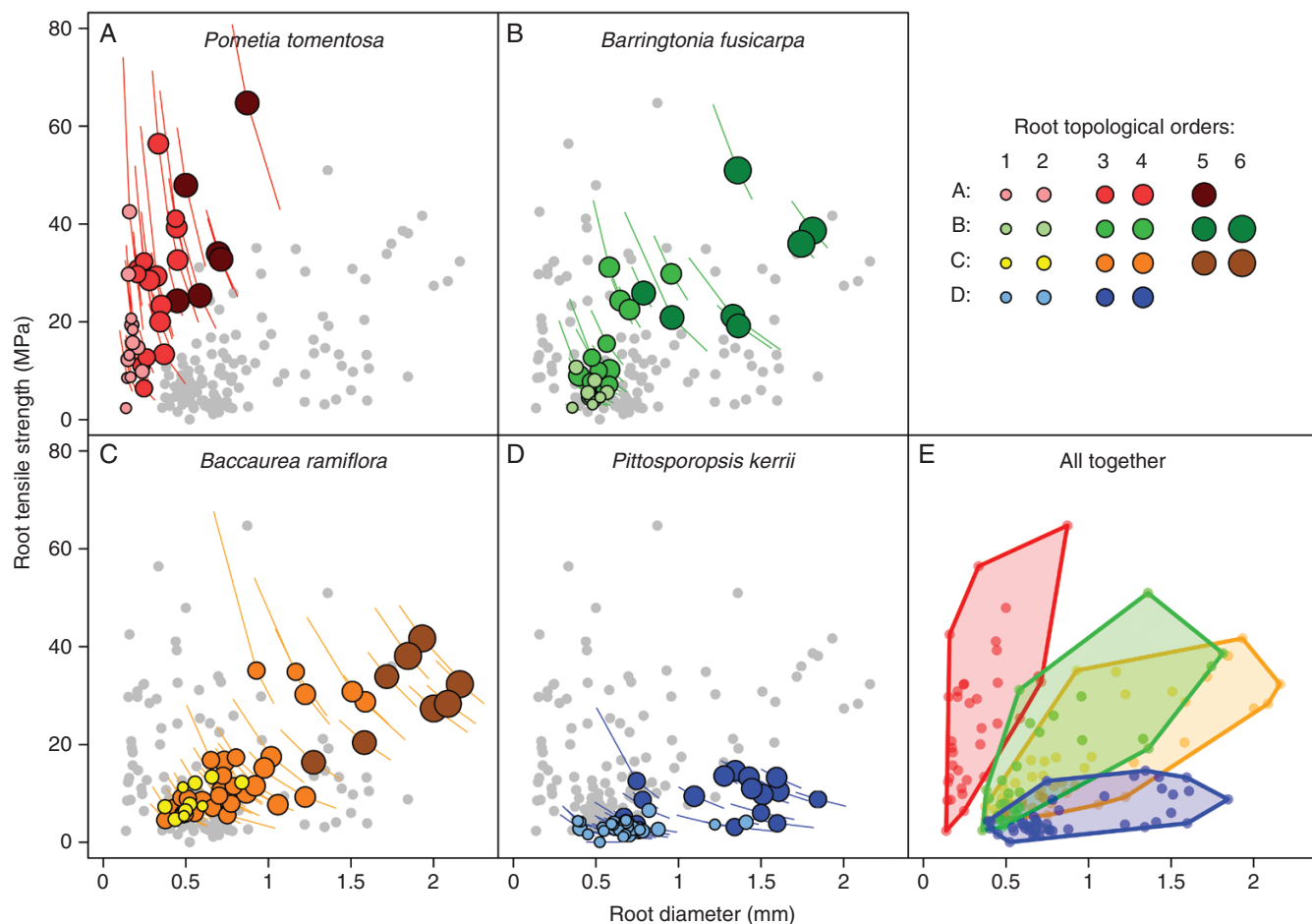
FIG. 2. Root tensile strength (T_r) as a function of diameter and topological order per species. (A–D) Inclined lines crossing points represent the uncertainties of the trait estimation due to the use of root diameter (d_{min} and d_{max}). (E) Points from the same species were grouped using convex hull polygons. Coloured symbols represent data for the species under consideration and grey symbols in the background (for better viewing) represent data values for the three remaining species.

although the patterns of these relationships differed somewhat. *F* exhibited an exponential increase with root diameter (Supplementary Data Fig. S1.3), while T_r increased roughly linearly (Fig. 2). The slight difference in the relationships of diameter with *F* and T_r was also well represented by the model fit in each species, the fitted coefficient *B* for *F* [in eqn (3)] is >2 (Supplementary Data Fig. S1.3), rendering β for T_r in eqn (4) positive. Roots <1 mm in diameter tended to have similar *F* (<20 N) regardless of species, but the species exhibited substantial differences among roots >1 mm in diameter (Supplementary Data Fig. S1.3). This result was most distinct when comparing *P. kerrii* with the other three species, as the convex hull morphospace was offset from that of the other species, each of which generally overlapped one another (Supplementary Data Fig. S1.3e). Unlike *F*, the convex hull plots between T_r and diameter differed widely among the four species (Fig. 2E). There was no overlap between convex hulls of *P. tomentosa* and *P. kerrii*, whereas the convex hulls between *B. fusicarpa* and *B. ramiflora* were partially overlapping but still fully distinguishable (Fig. 2E). The steepest positive slope of T_r with diameter was observed

for *P. tomentosa*, followed by *B. fusicarpa* > *B. ramiflora* > *P. kerrii*.

The relationship between E_r and diameter (Fig. 3) exhibited a pattern similar to that between T_r and diameter, and relationships between E_r and diameter were more similar among species than for T_r (Figs 2E and 3E). When comparing roots of similar diameters (e.g. 1.5–2.0 mm), *P. kerrii* had both the lowest T_r (<20 MPa) and the lowest E_r (<400 MPa). Among thinner roots, *P. tomentosa* developed mechanically stronger roots with a higher E_r (Figs 2A and 3A). Comparisons between species and root order showed that *P. kerrii* generally had higher diameter but lower T_r and E_r than those of the other species for the same root order (Table 2).

Our use of multiple measures of root diameter determined that relatively small measurement errors could lead to substantial variability in the estimates of T_r and E_r. Ultimately, calculating T_r and E_r based on the various measurements could alter estimates by up to 50 % in some extreme cases (error bars in Figs 2A–D and 3A–D). This potential for error was most noticeable in *P. tomentosa* but was more constrained in *P. kerrii*.
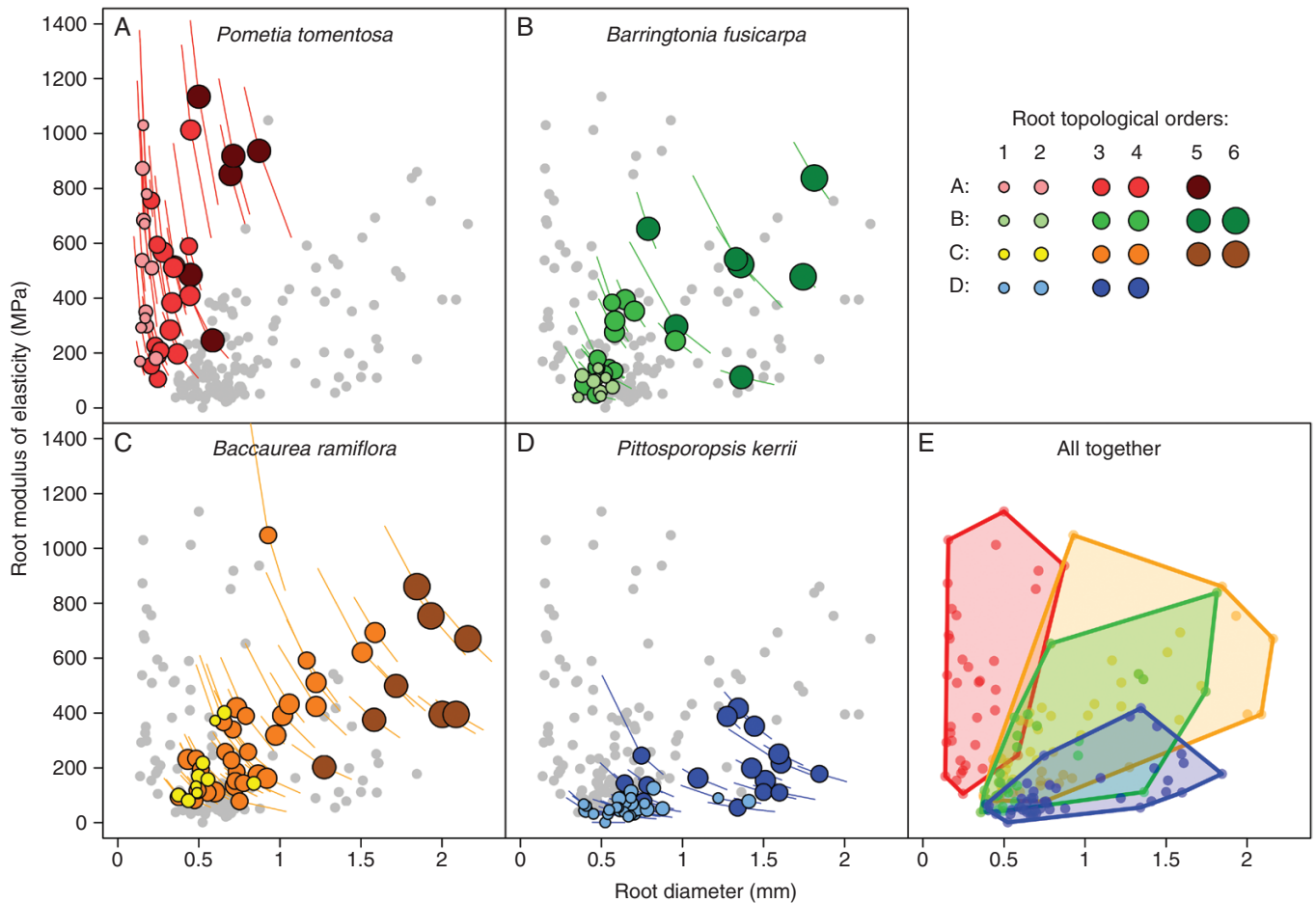
FIG. 3. Root modulus of elasticity (E_r) as a function of root diameter and topological order for each species. In (E), points from the same species were grouped using convex hull polygons. Coloured symbols represent data for the species under consideration and grey symbols in the background (for better viewing) represent data values for the three remaining species.

At the intraspecific level, root order and diameter were similar in their capacity to predict T_r and E_r depending on the study species (Table 1). By considering root order as a three-level qualitative variable (i.e. root orders 1–2, 3–4 and 5–6), linear regressions considering both diameter and order showed that both variables were significantly related to T_r (*B. fusicarpa* and *P. kerrii*) and E_r (*P. kerrii*), but only diameter was significantly related to T_r and E_r in *P. tomentosa* and *B. ramiflora* (Supplementary Data Table S1). When we considered diameter as a function of root order, the range of root diameters per order was highly variable among species, with the narrowest range found in *P. tomentosa* (~1 mm in all six orders) and the largest in *P. kerrii* (up to 2 mm in four orders) (Fig. 2A–D). At the interspecific level, the observed patterns in mechanical traits were better correlated with root order, not diameter, at the interspecific level (see Supplementary Data Fig. S1.4 for the example of T_r).

No clear patterns existed for ε_r as a function of root order or diameter (Fig. 4, Table 2) within any species. Most of the values for ε_r were <30 % (Fig. 4A–D), although *P. tomentosa* and *B. fusicarpa* tended to have greater variations in ε_r than did *B. ramiflora* and *P. kerrii*. Regarding the relationships between ε_r and root diameter and topological order among species, there were again only limited differences (Fig. 4E).

Root anatomical traits

Anatomical analyses for each of the four species showed that pentarchic xylem poles were observed in first- to third-order roots in *B. fusicarpa*, *B. ramiflora* and *P. kerrii*, but not in *P. tomentosa*. Secondary xylem first occurred in fourth-order roots in all species (data not shown; Fig. 5A). Within each species, first- and second-order roots often did not differ significantly in their root diameter and first- to third-order roots often possessed similar mechanical traits (Table 2). Stele diameter increased with increasing root order and diameter (Table 3, Fig. 5B). Cortex thickness also increased for the first three root orders in *P. tomentosa* and *B. fusicarpa* but then decreased in higher-order roots, while cortex thickness in *P. kerrii* and *B. ramiflora* remained more stable in the fourth and fifth root orders (Table 3). Stele area ratio was greater in higher-order roots, which was the opposite of the case for cortex diameter ratio (Table 3). Stele area ratio and cortex diameter ratio also varied among species. *Pometia tomentosa* roots had significantly larger stele areas but smaller cortex diameter ratios than the other three species (Table 3). Although *P. kerrii* tended to have the largest root diameters of the four species, its stele area ratio was significantly lower than that of *P. tomentosa* and comparable
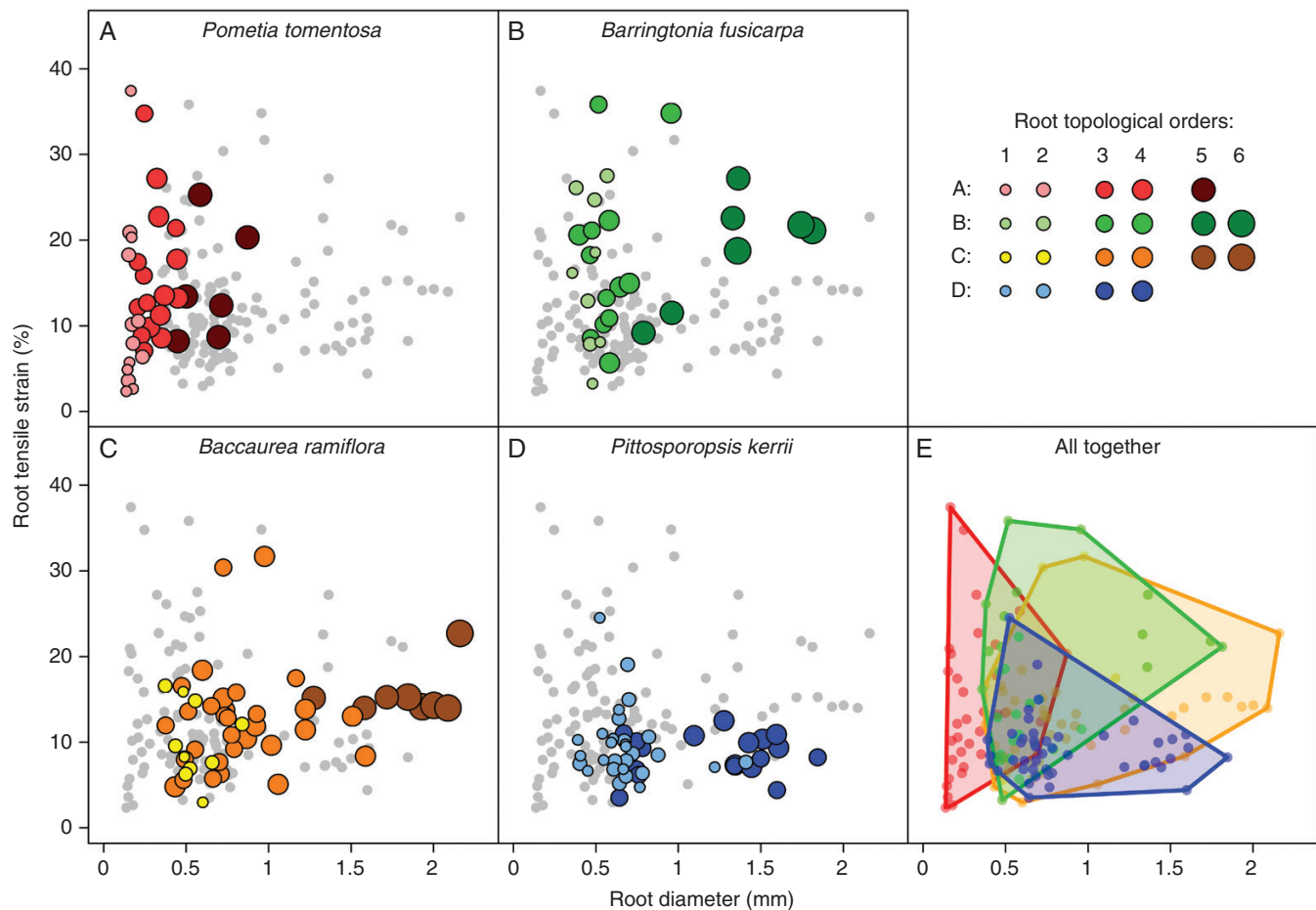
FIG. 4. Root tensile strain (ε_r) as a function of root diameter and topological order for each species. In (E), points from the same species were grouped using convex hull polygons. Coloured symbols represent data for the species under consideration and grey symbols in the background (for better viewing) represent data values for the three remaining species.

with those of *B. ramiflora* and *B. fusicarpa* (Table 3). *P. kerrii* had the greatest cortex diameter ratio among the four species.

Correlations between root traits at the interspecific level

The first axis of the PCA (Fig. 6) explained 61.4 % of the variation among all the factors and was mostly associated with F, T_r, E_r, root order, stele ratio and stele diameter. The second axis explained 26.0 % of the variation and was mostly associated with cortex thickness (Fig. 6). Similar to what was found at the intraspecific level, T_r and E_r were strongly correlated at the interspecific level (Fig. 6, Table 4). Both were positively correlated with topological order and stele area ratio. Stele area ratio better explained variations in T_r and E_r than did topological order or diameter (Table 4). Stele diameter better explained F than did root diameter, while topological order had comparable predictive capabilities. When considering all species together, topological order was often a better predictor of traits (especially T_r and E_r) than root diameter (Table 4, Fig. 6). Cortex thickness was independent of T_r and E_r, but it was indirectly related to mechanical strength through the cortex diameter ratio

(which was closely related to stele area ratio) and hence was negatively correlated to T_r and E_r.

At the intraspecific scale, ε_r was largely independent of T_r and E_r, and it could not be reasonably predicted by root diameter or topological order. However, at the interspecific scale, ε_r showed similar trends to T_r and E_r and was significantly and positively correlated with stele area ratio (Fig. 6).

DISCUSSION

Diameter and topological relationships to mechanical traits

Despite the importance of fine root mechanical traits in both empirical assessments of plant growth strategies and models of biophysical root–soil interactions, there is tremendous uncertainty regarding the factors contributing to the wide variation of these traits (Schwarz *et al.*, 2010; Mao *et al.*, 2014*a*, *b*). Root diameter has been shown to be an ineffective indicator of the variation encountered in mechanical traits of roots both within and among species (Ghestem *et al.*, 2014). In this study, we leverage a growing understanding of the role that topological order plays in defining root function, together with detailed

TABLE 2. *Means and standard errors of root diameter (*d*, mm), tensile strength (*T$_r$*, MPa), modulus of elasticity (*E$_r$*, MPa) and tensile strain (*ε$_r$*, %) for each root topological order*

Trait	Species	Root topological order					
		1	2	3	4	5	6
d	*P. tomentosa*	B 0.16 ± 0.01 a	C 0.18 ± 0.01 a	C 0.26 ± 0.03 ab	C 0.36 ± 0.02 b	B 0.64 ± 0.06 c	–
	B. fusicarpa	A 0.46 ± 0.04 a	B 0.47 ± 0.03 a	BC 0.52 ± 0.02 a	C 0.64 ± 0.08 a	A 1.11 ± 0.14 b	A 1.64 ± 0.14 c
	B. ramiflora	A 0.52 ± 0.04 a	AB 0.55 ± 0.06 a	B 0.68 ± 0.04 a	B 0.99 ± 0.09 b	A 1.52 ± 0.13 c	B 2.01 ± 0.06 c
	P. kerrii	A 0.62 ± 0.05 a	A 0.73 ± 0.06 a	A 1.06 ± 0.14 b	A 1.41 ± 0.06 b	–	–
F	*P. tomentosa*	A 0.26 ± 0.07 a	B 0.48 ± 0.07 a	A 1.59 ± 0.68 a	A 3.24 ± 0.65 a	B 14.12 ± 5.12 b	–
	B. fusicarpa	A 0.63 ± 0.16 a	AB 1.17 ± 0.14 a	A 1.98 ± 0.37 a	A 8.37 ± 2.91 a	AB 21.31 ± 4.32 b	A 86.59 ± 7.46 c
	B. ramiflora	A 1.73 ± 0.36 a	A 2.67 ± 0.86 a	A 6.36 ± 2.2 a	A 16.8 ± 5.38 a	A 46.45 ± 16.92 b	A 105.12 ± 6.74 c
	P. kerrii	A 0.96 ± 0.28 a	A 1.57 ± 0.39 a	A 6.18 ± 2.16 b	A 18.96 ± 1.78 c	–	–
T$_r$	*P. tomentosa*	B 11.98 ± 2.79 b	B 20.6 ± 4.38 ab	B 24.56 ± 4.46 ab	B 30.35 ± 4.65 ab	A 38.18 ± 6.34 a	–
	B. fusicarpa	A 3.46 ± 0.45 a	A 6.92 ± 1.09 a	A 9.23 ± 1.43 a	AB 21.17 ± 3.89 b	A 21.79 ± 1.44 b	A 41.86 ± 4.62 c
	B. ramiflora	AB 8.03 ± 1.72 a	A 9.15 ± 1.28 a	A 12.17 ± 2.14 a	A 15.53 ± 2.46 a	A 23.55 ± 5.29 a b	A 33.56 ± 2.78 b
	P. kerrii	A 2.78 ± 0.36 a	A 3.27 ± 0.31 a	A 5.78 ± 1.03 b	A 11.94 ± 0.70 c	–	–
E$_r$	*P. tomentosa*	B 545.19 ± 136.41 a	B 490.61 ± 89.83 a	A 353.35 ± 88.7 a	A 485.54 ± 87.27 a	A 762.16 ± 134.79 a	–
	B. fusicarpa	A 84.12 ± 26.19 a	A 90.25 ± 10.42 a	A 166.48 ± 39.4 ab	A 278.51 ± 44.52 ab	A 401.26 ± 121.69 bc	A 613.15 ± 113.36 c
	B. ramiflora	A 205.18 ± 84.09 ab	A 181.9 ± 40.36 a	A 270.85 ± 55.28 a	A 356.05 ± 51.84 ab	A 359.05 ± 85.82 ab	A 615.22 ± 94.76 b
	P. kerrii	A 49.26 ± 6.91 a	A 64.04 ± 7.14 a	A 122.56 ± 17.9 b	A 267.85 ± 36.69 c	–	–
ε$_r$	*P.tomentosa*	A 12.23 ± 5.73 a	A 11.13 ± 2.38 a	B 16.28 ± 3.10 a	A 15.52 ± 2.32 a	A 14.72 ± 2.76 a	–
	B.fusicarpa	A 11.53 ± 3.55 a	B 19.82 ± 3.96 a	B 16.88 ± 3.59 a	A 18.82 ± 3.99 a	A 17.62 ± 4.33 a	A 20.56 ± 0.92 a
	B.ramiflora	A 9.05 ± 3.75 a	A 10.56 ± 1.53 a	AB 12.32 ± 1.37 a	A 12.89 ± 1.89 a	A 14.81 ± 0.4 a	A 16.08 ± 1.67 a
	P.kerrii	A 10.06 ± 1.26 a	A 9.34 ± 0.97 a	A 7.5 ± 0.75 a	A 9.78 ± 0.65 a	–	–

In each *d*,*F*, *T$_r$*, *E$_r$*, *ε$_r$* – root topological order matrix, the letters represent the Tukey HSD test results across root orders (lower case letters after the values) and species (capital letters before the values).
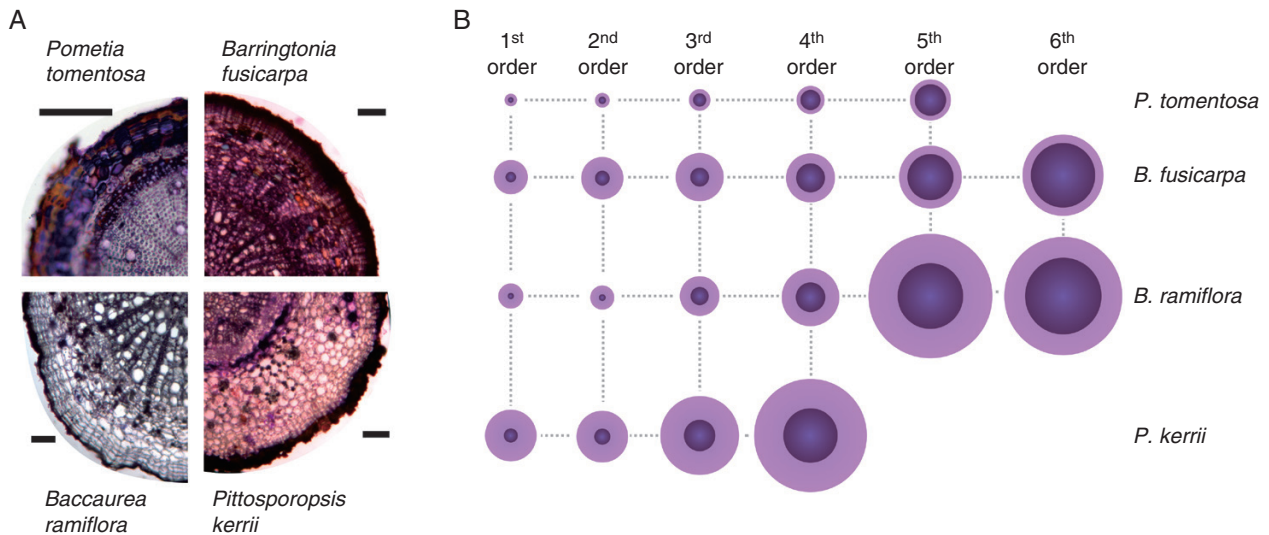

FIG. 5. Light microscope images of (A) cross-sections of fifth-order roots from *Pometia tomentosa*, *Barringtonia fusicarpa* and *Baccaurea ramiflora* and a fourth-order root from *Pittosporopsis kerrii*. Scale bar = 100 µm. (B) Line drawings showing representations of root size and cortex:stele ratio for all root orders. Light purple represents the cortex and dark purple represents the stele. Root and stele diameters were adjusted by the mean diameter for each corresponding order.

assessments of root morphology (diameter) and anatomy, to better explain patterns of strength and elasticity.

We found wide variation in three key mechanical traits (*T$_r$*, *ε$_r$* and *E$_r$*), with at least one order of magnitude difference between species as well as within species but across different root orders (Figs 2 and 3). We observed strong and positive increases in *T$_r$* and *E$_r$* with increasing diameter and this pattern was conserved within each of the four tree species (Figs 2 and 3). We also observed a strong positive relationship between diameter and *F*

across species, but there was no relationship with *T$_r$* across species. Nor did we observe a relationship between *ε$_r$* and diameter within or across species. Together, this led us to reject our first hypothesis – that *T$_r$*, *ε$_r$* and *E$_r$* would each be negatively related to root diameter.

Previous studies have often observed a positive quasi-linear relationship between *F* and root diameter and a negative power relationship between *T$_r$* and diameter (Hales *et al.*, 2009; Mao *et al.*, 2012; Giadrossich *et al.*, 2017). It is therefore expected

TABLE 3. *Means and standard errors of root diameter (mm), stele diameter (mm), cortex thickness (mm), stele ratio (mm²/mm²) and cortex ratio (mm/mm) for each root topological order*

Trait	Species	Root topological order					
		1	2	3	4	5	6
Diameter	*P. tomentosa*	C 0.18 ± 0.01 a	B 0.22 ± 0.01 a	B 0.31 ± 0.03 b	C 0.42 ± 0.01c	B 0.59 ± 0.04 d	–
	B. fusicarpa	B 0.49 ± 0.02 b	A 0.63 ± 0.05 ab	B 0.69 ± 0.04 ac	BC 0.73 ± 0.03 ac	B 0.90 ± 0.10 c	A 1.21 ± 0.03 d
	B. ramiflora	BC 0.36 ± 0.01 a	B 0.36 ± 0.01 a	B 0.57 ± 0.10 ab	B 0.86 ± 0.07 b	A 1.78 ± 0.15 c	A 1.76 ± 0.27 c
	P. kerrii	A 0.74 ± 0.05 b	A 0.77 ± 0.07 ab	A 1.13 ± 0.14 a	A 1.62 ± 0.18 c	–	–
Stele	*P. tomentosa*	C 0.08 ± 0.01 a	B 0.11 ± 0.01 a	B 0.19 ± 0.01 b	B 0.30 ± 0.01 c	B 0.45 ± 0.04 d	–
	B. fusicarpa	AB 0.15 ± 0.01 b	A 0.22 ± 0.02 ab	AB 0.27 ± 0.02 a	B 0.43 ± 0.05 c	B 0.66 ± 0.08 d	A 0.96 ± 0.01 e
	B. ramiflora	BC 0.09 ± 0.00 a	B 0.10 ± 0.00 a	AB 0.26 ± 0.08 ab	B 0.44 ± 0.05 b	A 0.94 ± 0.02 c	A 1.14 ± 0.17 c
	P. kerrii	A 0.20 ± 0.02 a	A 0.24 ± 0.02 a	A 0.45 ± 0.07 b	A 0.78 ± 0.07 c	–	–
Cortex thickness	*P. tomentosa*	C 0.04 ± 0.01 a	C 0.03 ± 0.00 a	C 0.04 ± 0.01 a	C 0.03 ± 0.00 a	B 0.02 ± 0.00 a	–
	B. fusicarpa	B 0.14 ± 0.01 a	B 0.16 ± 0.01 a	B 0.17 ± 0.01 a	BC 0.12 ± 0.02 ab	B 0.08 ± 0.01 b	A 0.07 ± 0.01 b
	B. ramiflora	B 0.12 ± 0.00 a	B 0.12 ± 0.01 a	B 0.13 ± 0.01 a	B 0.19 ± 0.01 ab	A 0.38 ± 0.06 c	B 0.28 ± 0.07 bc
	P. kerrii	A 0.24 ± 0.02 ab	A 0.22 ± 0.02 a	A 0.29 ± 0.04 ab	A 0.35 ± 0.06 b	–	–
Stele area ratio	*P. tomentosa*	B 0.18 ± 0.05 b	B 0.27 ± 0.03 ab	B 0.40 ± 0.04 ac	B 0.50 ± 0.02 c	B 0.57 ± 0.03 c	–
	B. fusicarpa	A 0.10 ± 0.01 a	A 0.13 ± 0.01 a	A 0.15 ± 0.01 a	A 0.35 ± 0.06 b	B 0.53 ± 0.02 c	A 0.64 ± 0.02 c
	B. ramiflora	A 0.06 ± 0.00 a	A 0.08 ± 0.01 a	A 0.18 ± 0.04 ab	A 0.26 ± 0.02 bc	A 0.30 ± 0.04 bc	B 0.42 ± 0.00 c
	P. kerrii	A 0.07 ± 0.01 a	A 0.10 ± 0.00 a	A 0.16 ± 0.02 b	A 0.25 ± 0.04c	–	–
Cortex diameter ratio	*P. tomentosa*	B 0.42 ± 0.05 b	C 0.32 ± 0.03 ab	B 0.23 ± 0.03 ac	B 0.15 ± 0.01 c	B 0.08 ± 0.01 c	–
	B. fusicarpa	A 0.56 ± 0.02 a	B 0.53 ± 0.02 a	A 0.50 ± 0.01 a	A 0.35 ± 0.06 b	B 0.18 ± 0.02 c	A 0.12 ± 0.01 c
	B. ramiflora	A 0.65 ± 0.01 a	A 0.65 ± 0.02 a	A 0.51 ± 0.04 b	A 0.44 ± 0.02 bc	A 0.42 ± 0.04 bc	B 0.31 ± 0.03 c
	P. kerrii	A 0.64 ± 0.01 c	A B 0.57 ± 0.01 a	A 0.51 ± 0.02 a	A 0.42 ± 0.04 b	–	–

In each trait–root topological order matrix, the letters represent the Tukey HSD test results across root orders (lower case letters after the values) and species (capital letters before the values).
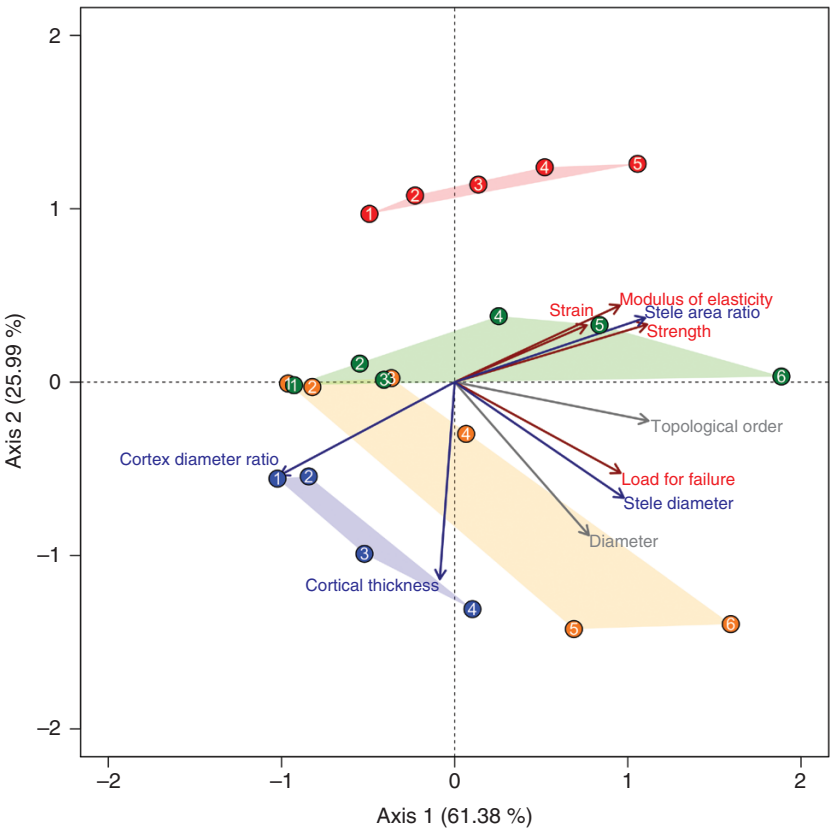

FIG. 6. Relationships between root traits described using principal component analysis. Arrow colours represent different types of traits (grey, morphological and architectural; dark blue, anatomical; dark red, mechanical). Each point corresponds to the assembly of averaged traits for each root topological order, which is given inside the point circle. Colours of symbols represent different species: red, *Pometia tomentosa*; green, *Barringtonia fusicarpa*; orange, *Baccaurea ramiflora*; blue, *Pittosporopsis kerrii*. Data from the same species were grouped using convex hull polygons.

TABLE 4. *Pearson correlation coefficients among root traits for all four species*

	TO	d	F	T_r	E_r	ε_r	SD	CT	SAR	CDR
Topological order (TO)										
Diameter (d)	0.62**									
Load for failure (F)	0.87***	0.88***								
Strength (T_r)	0.76***	0.16	0.60**							
Modulus of elasticity (E_r)	0.60**	0.04	0.47*	0.94***						
Strain (ε_r)	0.53*	0.09	0.36	0.62**	0.44*					
Stele diameter (SD)	0.86***	0.86***	0.92***	0.49*	0.33	0.39				
Cortex thickness (CT)	0.01	0.64**	0.30	−0.48*	−0.55*	−0.29	0.36			
Stele area ratio (SAR)	0.83***	0.24	0.61**	0.90***	0.81***	0.64**	0.65**	−0.43		
Cortex diameter ratio (CDR)	−0.63**	−0.09	−0.44*	−0.80***	−0.72***	−0.55**	−0.44*	0.67***	−0.88***	

All data were log-transformed to meet the normality assumption.

***$P < 0.001$; **$P < 0.01$; *$P < 0.05$.

that thicker roots can withstand greater loading due to their size, but that material properties are more resistant (higher T_r) in the smaller roots of a given root system. That is, on a per cross-sectional area basis, thinner roots were thought to be stronger than thicker roots. However, our results challenge the previous assumptions relating T_r and root diameter and we propose that differences in types of sampled roots are responsible for contrasting results. As we investigated root mechanical traits with an explicit consideration of topological order, we did not mix roots at different developmental stages. In previous studies where development was not considered, roots with different anatomical characteristics and chemical composition were grouped together into broad diameter classes (e.g. Mao *et al.*, 2012; Bischetti *et al.*, 2005, 2009; Genet *et al.*, 2005; Pollen and Simon, 2005; De Baets *et al.*, 2008; Fan and Su, 2008; Zhang *et al.*, 2014). Our findings suggest that T_r versus diameter curves should follow a unimodal shape rather than a conventionally described monotonic decreasing trend. For coarse and high-order roots, which are older than distal, fine roots, the consistently low T_r and E_r values can be explained by the classic imperfection theory in material mechanics (Timoshenko, 1956). This theory suggests that increasingly large roots have a higher probability of material defects occurring in either cellulose structuration or cell wall layer bonding, resulting in lower strength (Hathaway and Penny, 1975). Regarding the younger, more distal roots, especially first- to third-order roots, the low T_r values are likely due to the early developmental stage of tissue, which has a low lignification level and smaller stele area ratio, resulting in the expression of relatively weak tissues among lower root orders, which coincide with smaller diameters.

We found no clear intraspecific relationships between ε_r and root diameter or topological order. However, with increasing diameter the variability in ε_r tended to decrease. Overall, the absence of clear, intraspecific patterns and lack of relationships with other mechanical traits (T_r and E_r) among species suggests that variations in ε_r are likely related to other factors, such as root cell length and cell wall microstructure, as in stem wood (Flores and Friswell, 2013). Tensile strain is also highly dependent on the quality of laboratory tests and of the sample. Aside from slippage of a root in the clamps occurring during a test (which can be avoided or amended), biological materials such as roots are subject to natural variations in shape, especially with regard to straightness or tortuosity

(Commandeur and Pyles, 1991). During a tensile test, the initial stretching phase will differ in magnitude depending on how much a tortuous root must be stretched before the elastic and plastic phases of deformation occur. Further studies therefore need to be carried out to better understand these effects of tortuosity on tensile strain and the consequences for root mechanical traits.

Anatomical drivers of root mechanical strength

In support of our second hypothesis, variation in root anatomical traits was a strong predictor of variation in root mechanical properties both within and across species. Increases in T_r and E_r were most closely related to larger stele size, whereas a thicker cortex was associated with mechanically weak roots. Chimungu *et al.* (2015) also found that, within a given species, stele diameter was a better predictor of root tensile strength than diameter. Root strain (ε_r), which was poorly correlated with other root traits at the intraspecific level, was positively related with stele area ratio at the interspecific level, suggesting that stele area ratio plays a broadly important role in defining the variability of root mechanics among species. This phenomenon was most clearly indicated by comparing *P. tomentosa* with other species, as the higher stele area ratios of *P. tomentosa* were consistently related to higher mechanical strength for a given root order despite their smaller diameters. While the stele provides mechanical robustness and is responsible for water and solute transport (Katou *et al.*, 1987), the root cortex plays an essential role in mycorrhizal associations (Brundrett, 2002) and water and nutrient absorption from soil (Peterson *et al.*, 1999). Differences in cortex:stele thickness ratios between species may therefore represent a functional trade-off among species or individuals, with higher cortex:stele ratios favouring higher resource acquisition rates with a greater cortex area, whereas lower ratios favour stronger roots that better resist mechanical damage and failure. Within a species, this trade-off becomes clearer as there is a steady increase in stele area ratio and decrease in the cortex:diameter ratio moving from lower- to higher-order roots. This phenomenon largely signifies the transition of primary root function from a more absorptive role among lower-order roots to a more transport/storage based function in higher-order roots (McCormack *et al.*, 2015).

Root diameter and topology as predictors of mechanical traits

Root mechanical strength was related to topological order and, to a certain extent, diameter. Therefore, both these morphological traits act as tractable proxies to represent key changes in root anatomy and their effects on mechanical strength. Compared with anatomical traits that are more time-consuming to measure, both topological order and diameter are relatively simple to measure and thus can be considered good candidates for predicting T_r and E_r. Diameter has already been widely used as a proxy for root anatomy and predictor of mechanical traits (Mao *et al.*, 2012; Loades *et al.*, 2015). However, to our knowledge, no studies have previously investigated the potential for root topology to contribute to a better understanding of root mechanical trait variation, either on its own or in conjunction with root diameter. Our data show that root topological order is a comparable (at intraspecific level) or better (at interspecific level) predictor of mechanical traits than diameter, thus validating our third hypothesis. Nevertheless, measurements of topological order may be biased if root system architecture is not fully intact, therefore necessitating the excavation of entire portions of root systems, which can be labour-intensive (McCormack *et al.*, 2015). Furthermore, both root diameter and topological order together provided valuable information for understanding mechanical traits of the tree species used in our study. For example, jointly using diameter and topological order in regression models improved the model fit (e.g. R^2 increased by >0.1 for T_r in *P. kerrii* when incorporating topological order with diameter as opposed to using diameter or topological order alone, despite a higher Akaike information criterion value). Logically, topological order should best reflect differences within a species, as it captures aspects of root development that may be missed by diameter alone. Conversely, diameter may best reflect variation among species, as diameter and related functional traits can vary widely across species within the same topological order.

Practical applications

Data on tree root strength and elasticity are important for engineers, foresters and urban arborists. Root density and tensile strength determine the maximum mechanical resistance of a rooted soil, while elasticity and strain (E_r and ε_r) are used to determine root rigidity and the temporal behaviour of roots during mobilization (e.g. how far roots can stretch before failing during a landslide or tree overturning). To reinforce soil, an ideal species is expected to simultaneously develop fine roots with high T_r and E_r and a low ε_r for a given root size and quantity (Stokes *et al.*, 2009; Ghestem *et al.*, 2014), e.g. *P. tomentosa* and *B. fusicarpa* in our study. The generally synergistic relationship among F, T_r and E_r within species may facilitate optimal species selection if researchers are unable to characterize each trait individually. In our study we showed that root strain (ε_r) was highly variable in each species but generally had relatively low values (<30 %) in all four species. Compared with F, T_r and E_r, the low variation in ε_r among species would suggest that ε_r may be a less important criterion for species selection compared with tensile strength and elasticity.

Conclusions

We identified consistent patterns of root mechanical trait variation at two levels. At the intraspecific level, we rejected our initial hypothesis by finding that root diameter and topological order were positively related to all of the measured mechanical traits except strain. When considering both the intra- and interspecific level, topological order was a better predictor than root diameter in explaining the variability of tensile strength and modulus of elasticity. Root strength and elasticity were also more closely related to stele development, than cortex thickness. Accordingly, topological order was better correlated to stele area ratio than was root diameter.

Our study has implications for future research on tree, shrub and herbaceous species. Both woody and herbaceous plants play important roles in slope stabilization and in reducing soil erosion. In urban ecosystems or plantations, root tensile strength is related to the likelihood of uprooting during wind storms. Many herbaceous plants are also subjected to additional tensile forces associated with grazing, yet mechanical traits are rarely included in most studies of plant function and ecology. Future work incorporating root mechanical traits into functional ecology while also considering root system topology and morphology will enable better understanding of plant growth and functioning at both the individual and the community level.

SUPPLEMENTARY DATA

Supplementary data are available online at https://academic.oup.com/aob and consist of the following. Table S1.1: linear regressions on root mechanical traits using both root diameter and topological order in the model. Figure S1.1: comparison of measured diameters (mean ± s.e.) between two sources of roots (those for mechanical tests versus those for anatomical measurements). Figure S1.2: difference in root diameter per root topological order between the roots sampled for mechanical tests and those for anatomical measurements. Figure S1.3: load to failure in tension as a function of root diameter and topological order per species. Figure S1.4: interspecific variation of root tensile strength (T_r) as a function of root diameter (d, x-axis) and topological order (convex hull polygons).

ACKNOWLEDGEMENTS

logistical support. We thank Cheng'en Ma (IGSNRR-CAS) for his suggestions concerning the fieldwork.

LITERATURE CITED

De Baets S, **Poesen J**, **Reubens B**, **Wemans K**, **De Baerdemaeker J**, **Muys B.** **2008**. Root tensile strength and root distribution of typical Mediterranean plant species and their contribution to soil shear strength. *Plant and Soil* **305**: 207–226.

Berntson GM. 1997. Topological scaling and plant root system architecture: developmental and functional hierarchies. *New Phytologist* **135**: 621–634.

Bischetti GB, **Chiaradia EA**, **Simonato T**, *et al.* **2005**. Root strength and root area ratio of forest species in Lombardy (Northern Italy). *Plant and Soil* **278**: 11–22.

Bischetti GB, **Chiaradia EA**, **Epis T**, **Morlotti E. 2009**. Root cohesion of forest species in the Italian Alps. *Plant and Soil* **324**: 71–89.

Bourrier F, **Kneib F**, **Chareyre B**, **Fourcaud T. 2013**. Discrete modeling of granular soils reinforcement by plant roots. *Ecological Engineering* **61**: 646–657.

Brundrett MC. 2002. Coevolution of roots and mycorrhizas of land plants. *New Phytologist* **154**: 275–304.

Cao M, **Zou X**, **Warren M**, **Zhu H. 2006**. Tropical forests of Xishuangbanna, China. *Biotropica* **38**: 306–309.

Chimungu JG, **Loades KW**, **Lynch JP. 2015**. Root anatomical phenes predict root penetration ability and biomechanical properties in maize (*Zea mays*). *Journal of Experimental Botany* **66**: 3151–3162.

Commandeur PR, **Pyles MR. 1991**. Modulus of elasticity and tensile strength of Douglas-fir roots. *Canadian Journal of Forest Research* **21**: 48–52.

Cormen TH, **Leiserson CE**, **Rivest RL**, **Stein C. 2001**. *Introduction to algorithms*, 2nd edn. Cambridge, MA: MIT Press, 947–957.

Domec JC, **Gartner BL. 2002**. Age- and position-related changes in hydraulic versus mechanical dysfunction of xylem: inferring the design criteria for Douglas-fir wood structure. *Tree Physiology* **22**: 91–104.

Denny M, **Gaylord B. 2002**. The mechanics of wave-swept algae. *Journal of Experimental Biology* **205**: 1355–1362.

Fan CC, **Su CF. 2008**. Role of roots in the shear strength of root-reinforced soils with high moisture content. *Ecological Engineering* **33**: 157–166.

Fitter AH. 1982. Morphometric analysis of root systems: application of the technique and influence of soil fertility on root system development in two herbaceous species. *Plant, Cell & Environment* **5**: 313–322.

Flores EIS, **Friswell MI. 2013**. Ultrastructural mechanisms of deformation and failure in wood under tension. *International Journal of Solids & Structures* **50**: 2050–2060.

Genet M, **Stokes A**, **Salin F**, *et al.* **2005**. The influence of cellulose content on tensile strength in tree roots. *Plant and Soil* **278**: 1–9.

Genet M, **Li MC**, **Luo TX**, **Fourcaud T**, **Clement-Vidal A**, **Stokes A. 2011**. Linking carbon supply to root cell-wall chemistry and mechanics at high altitudes in *Abies georgei*. *Annals of Botany* **107**: 311–320.

Giadrossich F, **Schwarz M**, **Cohen D**, *et al.* **2017**. Methods to measure the mechanical behaviour of tree roots: a review. *Ecological Engineering* **109**: 256–271.

Ghestem M, **Cao K**, **Ma W**, *et al.* **2014**. A framework for identifying plant species to be used as 'ecological engineers' for fixing soil on unstable slopes. *PLoS One* **9**: e95876.

Guo DL, **Mitchell RJ**, **Hendricks JJ. 2004**. Fine root branch orders respond differentially to carbon source-sink manipulations in a longleaf pine forest. *Oecologia* **140**: 450–457.

Guo DL, **Xia M**, **Wei X**, **Chang W**, **Liu Y**, **Wang Z. 2008**. Anatomical traits associated with absorption and mycorrhizal colonization are linked to root branch order in twenty-three Chinese temperate tree species. *New Phytologist* **180**: 673–683.

Hales TC, **Ford CR**, **Hwang T**, **Vose JM**, **Band LE. 2009**. Topographic and ecologic controls on root reinforcement. *Journal of Geophysical Research: Earth Surface* **114**: FO3013.

Hathaway RL, **Penny D. 1975**. Root strength in some *Populus* and *Salix* clones. *New Zealand Journal of Botany* **13**: 333–344.

Hishi T. 2007. Heterogeneity of individual roots within the fine root architecture: causal links between physiological and ecosystem functions. *Journal of Forest Research* **12**: 126–133.

Iversen CM, **McCormack ML**, **Powell AS**, *et al.* **2017**. A global Fine-Root Ecology Database to address below-ground challenges in plant ecology. *New Phytologist* **215**: 15–26.

Jacobsen AL, **Agenbag L**, **Esler KJ**, **Pratt RB**, **Ewers FW**, **Davis SD. 2007**. Xylem density, biomechanics and anatomical traits correlate with water stress in 17 evergreen shrub species of the Mediterranean-type climate region of South Africa. *Journal of Ecology* **95**: 171–183.

Johnson SN, **Erb M**, **Hartley SE. 2016**. Roots under attack: contrasting plant responses to below- and aboveground insect herbivory. *New Phytologist* **210**: 413–418.

Katou K, **Taura T**, **Furumoto M. 1987**. A model for water transport in the stele of plant roots. *Protoplasma* **140**: 123–132.

Kong D, **Ma C**, **Zhang Q**, *et al.* **2014**. Leading dimensions in absorptive root trait variation across 96 subtropical forest species. *New Phytologist* **203**: 863–872.

Loades KW, **Bengough AG**, **Bransby MF**, **Hallett PD. 2013**. Biomechanics of nodal, seminal and lateral roots of barley: effects of diameter, waterlogging and mechanical impedance. *Plant and Soil* **370**: 407–418.

Loades KW, **Bengough AG**, **Bransby MF**, **Hallett PD. 2015**. Effect of root age on the biomechanics of seminal and nodal roots of barley (*Hordeum vulgare* L.) in contrasting soil environments. *Plant and Soil* **395**: 253–261.

Ma Z, **Guo D**, **Xu X**, *et al.* **2018**. Evolutionary history resolves global organization of root functional traits. *Nature* **555**: 94–97.

Mao Z, **Saint-André L**, **Genet M**, *et al.* **2012**. Engineering ecological protection against landslides in diverse mountain forests: choosing cohesion models. *Ecological Engineering* **45**: 55–69.

Mao Z, **Yang M**, **Bourrier F**, **Fourcaud T. 2014*a***. Evaluation of root reinforcement models using numerical modelling approaches. *Plant and Soil* **381**: 249–270.

Mao Z, **Bourrier F**, **Stokes A**, **Fourcaud T. 2014*b***. Three-dimensional modelling of slope stability in heterogeneous montane forest ecosystems. *Ecological Modelling* **273**: 11–22.

McCormack ML, **Dickie IA**, **Eissenstat DM**, *et al.* **2015**. Redefining fine roots improves understanding of below-ground contributions to terrestrial biosphere processes. *New Phytologist* **207**: 505–518.

Niklas KJ. 1992. *Plant biomechanics: an engineering approach to plant form and function*. Chicago: University of Chicago Press.

Niklas KJ. 1999. Variations of the mechanical properties of *Acer saccharum* roots. *Journal of Experimental Biology* **50**: 193–200.

Niklas KJ, **Molina-Freaner F**, **Tinoco-Ojanguren C**, **Paolillo DJ Jr**. **2002**. The biomechanics of *Pachycereus pringlei* root systems. *American Journal of Botany* **89**: 12–21.

Onoda Y, **Westoby M**, **Adler PB**, *et al.* **2011**. Global patterns of leaf mechanical properties. *Ecology Letters* **14**: 301–312.

Osnas JL, **Lichstein JW**, **Reich PB**, **Pacala SW. 2013**. Global leaf trait relationships: mass, area, and the leaf economics spectrum. *Science* **340**: 741–744.

Peterson CA, **Enstone DE**, **Taylor JH. 1999**. Pine root structure and its potential significance for root function. *Plant and Soil* **217**: 205–213.

Pollen N, **Simon A. 2005**. Estimating the mechanical effects of riparian vegetation on stream bank stability using a fiber bundle model. *Water Resources Research* **41**: W07025.

Pratt RB, **Jacobsen AL**, **Ewers FW**, **Davis SD. 2007**. Relationships among xylem transport, biomechanics and storage in stems and roots of nine Rhamnaceae species of the California chaparral. *New Phytologist* **174**: 787–798.

Pregitzer KS, **Kubiske ME**, **Yu CK**, **Hendrick RL. 1997**. Relationships among root branch order, carbon, and nitrogen in four temperate species. *Oecologia* **111**: 302–308.

R Core Team. **2015**. *R: a language and environment for statistical computing*. Vienna: R Foundation for Statistical Computing. https://www.R-project.org/.

Read J, **Stokes A. 2006**. Plant biomechanics in an ecological context. *American Journal of Botany* **93**: 1546–1565.

Reich PB, **Walters MB**, **Ellsworth DS. 1991**. Leaf age and season influence the relationships between leaf nitrogen, leaf mass per area and photosynthesis in maple and oak trees. *Plant, Cell & Environment* **14**: 251–259.

Roumet C, **Birouste M**, **Picon-Cochard C**, *et al.* **2016**. Root structure–function relationships in 74 species: evidence of a root economics spectrum related to carbon economy. *New Phytologist* **210**: 815–826.

Schneider CA, **Rasband WS**, **Eliceiri KW. 2012**. NIH Image to ImageJ: 25 years of image analysis. *Nature Methods* **9**: 671–675.

Schwarz M, **Lehmann P**, **Or D. 2010**. Quantifying lateral root reinforcement in steep slopes – from a bundle of roots to tree stands. *Earth Surface Processes and Landforms* **35**: 354–367.

Schwarz M, **Rist A**, **Cohen D**, *et al.* **2015**. Root reinforcement of soils under compression. *Journal of Geophysical Research: Earth Surface* **120**: 2103–2120.

Stokes A, **Atger C**, **Bengough AG**, **Fourcaud T**, **Sidle RC. 2009**. Desirable plant root traits for protecting natural and engineered slopes against landslides. *Plant and Soil* **324**: 1–30.

Timoshenko SP. 1956. *Strength of materials, part II, advanced theory and problems, D*. Vol. **210**, 3rd edn. New York: Van Nostrand Company.

Violle C, **Navas ML**, **Vile D**, *et al.* **2007**. Let the concept of trait be functional! *Oikos* **116**: 882–892.

Wagner KR, **Ewers FW**, **Davis SD. 1998**. Tradeoffs between hydraulic efficiency and mechanical strength in the stems of four co-occurring species of chaparral shrubs. *Oecologia* **117**: 53–62.

Wang WF, **Qiu DY**, **Wu JC**, **Ye HM. 1996**. *The soils of Yunnan*. Kunming, China: Yunnan Science and Technology Press.

Woodrum CL, **Ewers FW**, **Telewski FW. 2003**. Hydraulic, biomechanical, and anatomical interactions of xylem from five species of *Acer* (Aceraceae). *American Journal of Botany* **90**: 693–699.

Wright IJ, **Westoby M. 2002**. Leaves at low versus high rainfall: coordination of structure, lifespan and physiology. *New Phytologist* **155**: 403–416.

Wright IJ, **Reich PB**, **Westoby M**, *et al.* **2004**. The worldwide leaf economics spectrum. *Nature* **428**: 821–827.

Wu TH, **McKinnell WP**, **Swanston DN. 1979**. Strength of tree roots and landslides on Prince of Wales Island, Alaska. *Canadian Geotechnical Journal* **16**: 19–33.

Zhang CB, **Chen LH**, **Jiang J. 2014**. Why fine tree roots are stronger than thicker roots: the role of cellulose and lignin in relation to slope stability. *Geomorphology* **206**: 196–202.